Journal of Applied Mathematics and Physics (ZAMP)
Vol. 40, November 1989

0044-2275/89/060846-26 $ 1.50 + 0.20

A time integration procedure for plastic deformation in elastic-viscoplastic metals

By M. B. Rubin, Faculty of Mechanical Engineering, Technion—Israel Institute of Technology, Haifa, Israel

1. Introduction

Classical theories of plastic flow in metals use a yield function to separate elastic and plastic response and assume that the flow stress is independent of strain rate [1]. Even if one is analyzing a dynamic problem where the flow stress is substantially increased relative to the static value, such theories may often be used if the strain rate experienced by the metal during the relevant portion of the process does not vary by more than about an order of magnitude. However, if the range of strain rate spans a few orders of magnitude then a more accurate model of strain-rate effects may be necessary. Knowledge of the temperature during the process is also important since strain-rate sensitivity tends to increase with increase in temperature.

Malvern [2] studied the influence of strain-rate sensitivity on wave propagation and introduced a model which is now called the overstress model. This overstress model retains the notion of a yield function which distinctly separates elastic and plastic response. However, it introduces strain-rate sensitivity by abandoning the consistency condition and allowing the yield function to be positive during plastic loading. Furthermore, the magnitude of plastic strain rate vanishes when the yield function vanishes and depends on the positive value of the yield function during plastic flow. Perzyna [3] generalized this model for the linear three-dimensional theory.

Another class of constitutive equations for elastic-viscoplastic materials abandons the notion of a yield function and assumes that plastic strain rate depends on the current state of the material. Unified constitutive equations for creep and plasticity of this type have been recently reviewed [4]. A common example of this type of constitutive equation is the power law model used by material scientists [5]. Another example which is of particular interest in this paper is the model proposed by Bodner and Partom [6, 7] and Bodner [8, 9]. This latter class of constitutive equations has been generalized to be consistent with continuum thermodynamics for large deformation including high compression [10, 11, 12].

In order to model the elastic response exhibited by metals for low stress levels, the flow rule proposed in a unified theory necessarily requires plastic strain-rate to be a highly nonlinear function of stress. Furthermore, since stress depends directly on plastic strain it follows that the flow rule yields stiff differential equations. Special numerical methods [13] have been developed to help stabilize the integration procedure. However, these numerical procedures become less effective as the material becomes less rate-sensitive because the flow rule becomes stiffer. In contrast, simple stable procedures using a yield function have been developed by Wilkins [14] and Maenchen and Sack [15] to integrate the flow rule for elastic-perfectly-plastic rate-insensitive materials. This method has been generalized by Krieg and Key [16] to include isotropic and kinematic strain hardening.

The objective of this paper is to develop a simple unconditionally stable numerical procedure for integrating the flow rule proposed by Rubin [12] which characterizes plastic deformation in an elastic-viscoplastic model exhibiting continuity of solid and fluid states. It is shown that this procedure remains simple even in the limit that the material response is nearly rate-insensitive.

In the following sections we record the basic constitutive equations for an elastic-viscoplastic metal. After presenting the numerical procedure, the problem of compression and shear is formulated and an exact analytical solution for steady state flow in simple shear is developed. The accuracy of the numerical procedure is examined relative to this exact solution. In addition, numerical examples of a corner test exhibiting the transition from uniaxial compression to simple shear, and a simple tension test are presented. Finally, an appendix is provided which records the basic equations associated with the small deformation theory.

2. Basic equations

For our present purpose we record the constitutive equations which were presented in [12] and which were modified slightly in [17] and later [18] shown to remain form invariant under change of the reference configuration. By way of background, let $\mathbf{X}$ denote the position of a material point in the reference configuration and let $\mathbf{x}$ denote the position of the same material point in the present configuration at time t. Also, let $\mathbf{F} = \partial \mathbf{x}/\partial \mathbf{X}$ be the deformation gradient; $\mathbf{C} = \mathbf{F}^T\mathbf{F}$ be the total deformation; $\mathbf{C}_p$ be a symmetric positive definite tensor denoting the plastic deformation; and θ be the absolute temperature.

Following Rubin [17] we introduce a multiplicative separation of elastic and plastic deformations and define the elastic deformation gradient $\mathbf{\Phi}_e$ and related kinematics by

$$\mathbf{M}_p = \mathbf{M}_p^T = \mathbf{C}_p^{1/2}, \quad \mathbf{\Phi}_e = \mathbf{F}\mathbf{M}_p^{-1}, \tag{2.1a,b}$$

$$\mathbf{C}_e = \mathbf{\Phi}_e^T\mathbf{\Phi}_e = \mathbf{M}_p^{-1}\mathbf{C}\mathbf{M}_p^{-1}, \quad \mathbf{B}_e = \mathbf{\Phi}_e\mathbf{\Phi}_e^T = \mathbf{F}\mathbf{C}_p^{-1}\mathbf{F}^T. \tag{2.1c,d}$$

We emphasize that the definition (2.1b) is significantly different from that introduced by Lubarda and Lee [19] since $\mathbf{M}_p$ and the resulting $\mathbf{C}_e$ are trivially invariant under superposed rigid body motions. Furthermore, it was noted in [17] that Green and Naghdi [20] introduced a tensor ($\mathbf{R}_p^T\mathbf{C}_e\mathbf{R}_p$ in their notation) equivalent to $\mathbf{C}_e$ in their analysis of the invariance properties of the separation of the deformation gradient proposed by Lee [21].

In general the elastic deformation tensors $\mathbf{C}_e$ and $\mathbf{B}_e$ may be separated into a pure measure of elastic dilatation I_{3e} and pure measures of elastic distortion $\mathbf{C}_e'$ and $\mathbf{B}_e'$ such that

$$I_{3e} = \det \mathbf{C}_e = \det \mathbf{B}_e = I_3/I_{3p}, \tag{2.2a}$$

$$\mathbf{C}_e' = I_{3e}^{-1/3}\mathbf{C}_e, \quad \mathbf{B}_e' = I_{3e}^{-1/3}\mathbf{B}_e, \tag{2.2b,c}$$

$$\det \mathbf{C}_e' = 1, \quad \det \mathbf{B}_e' = 1, \tag{2.2d,e}$$

where the total dilatation I_3 and the plastic dilatation I_{3p} are defined by

$$I_3 = \det \mathbf{C}, \quad I_{3p} = \det \mathbf{C}_p. \tag{2.3a,b}$$

Then, the condition of plastic incompressibility becomes

$$I_{3p} = 1, \quad I_{3e} = I_3. \tag{2.4a,b}$$

Furthermore, we note that although Rubin [11, 12, 17, 22] independently introduced the exact separation into dilatational and distortional deformations for plasticity (with elasticity as a special case), Flory [23] was the first to do so for elasticity and Simo *et al.* [24] were the first to do so for plasticity.

Following Rubin [12, 17] we specify the specific (per unit mass) Helmholtz free energy ψ and the entropy flux per unit reference area $\mathbf{P}$ by

$$\psi = \psi(I_3, \beta_1, \beta_2, \theta), \tag{2.5a}$$

$$\mathbf{P} = -[K(I_3, \beta_1, \beta_2, \theta)/\theta]I_3^{1/2}\mathbf{C}^{-1}\mathbf{G}, \tag{2.5b}$$

where β_1, β_2 are pure measures of elastic distortion related to the nontrivial invariants of $\mathbf{C}_e'$ and $\mathbf{B}_e'$, and $\mathbf{G}$ is the temperature gradient defined by

$$\beta_1 = \mathbf{C}_e'^{-1}\cdot\mathbf{I} = \mathbf{B}_e'^{-1}\cdot\mathbf{I} = I_3^{1/3}\mathbf{C}^{-1}\cdot\mathbf{C}_p, \tag{2.6a}$$

$$\beta_2 = \mathbf{C}_e'^{-1}\cdot\mathbf{C}_e'^{-1} = \mathbf{B}_e'^{-1}\cdot\mathbf{B}_e'^{-1} = I_3^{2/3}\mathbf{C}_p\mathbf{C}^{-1}\cdot\mathbf{C}^{-1}\mathbf{C}_p, \tag{2.6b}$$

$$\mathbf{G} = \partial\theta/\partial\mathbf{X}. \tag{2.6c}$$

Throughout the text the unit tensor is denoted by $\mathbf{I}$, and the notation $\mathbf{A} \cdot \mathbf{B} = \mathrm{tr}(\mathbf{A}\mathbf{B}^T)$ denotes the inner product between two second order tensors $\mathbf{A}$, $\mathbf{B}$.

Using the procedures proposed by Green and Naghdi [25, 26] and the results in [12] it can be shown that for the class of materials under consideration, the specific entropy η, the pressure p, the symmetric Piola-Kirchhoff stress $\mathbf{S}$, and the specific rate of entropy production ξ are given by

$$\eta = -\partial\psi/\partial\theta, \quad p = -2\varrho_0 I_3^{1/2}(\partial\psi/\partial I_3), \tag{2.7a,b}$$

$$\mathbf{S} = -pI_3^{1/2}\mathbf{C}^{-1} + \mathbf{S}', \quad \mathbf{S}' \cdot \mathbf{C} = 0, \tag{2.7c,d}$$

$$\begin{aligned}\mathbf{S}' = &-2\varrho_0 I_3^{1/3}(\partial\psi/\partial\beta_1)[\mathbf{C}^{-1}\mathbf{C}_p\mathbf{C}^{-1} - (\mathbf{C}_p \cdot \mathbf{C}^{-1}/3)\mathbf{C}^{-1}] \\ &- 4\varrho_0 I_3^{2/3}(\partial\psi/\partial\beta_2)[\mathbf{C}^{-1}\mathbf{C}_p\mathbf{C}^{-1}\mathbf{C}_p\mathbf{C}^{-1} \\ &- (\mathbf{C}_p\mathbf{C}^{-1} \cdot \mathbf{C}^{-1}\mathbf{C}_p/3)\mathbf{C}^{-1}]\end{aligned} \tag{2.7e}$$

$$\varrho_0\theta\xi = -\mathbf{P} \cdot \mathbf{G} + \varrho_0\theta\xi', \quad \varrho_0\theta\xi' = (1/2)(\mathbf{C}_p^{-1}\mathbf{C})\mathbf{S}' \cdot \dot{\mathbf{C}}_p, \tag{2.7f,g}$$

where ϱ_0 is the mass density in the reference configuration. Since the Cauchy stress $\mathbf{T}$ may be separated into a pressure p and a deviatoric part $\mathbf{T}'$

$$\mathbf{T} = p\mathbf{I} + \mathbf{T}', \quad \mathbf{T}' \cdot \mathbf{I} = 0, \tag{2.8a,b}$$

$$\mathbf{T}' = I_3^{-1/2}\mathbf{F}\mathbf{S}'\mathbf{F}^T, \tag{2.8c}$$

it follows from (2.1), (2.4), (2.7) and (2.8) that $\mathbf{T}'$ may be rewritten in the form

$$\begin{aligned}\mathbf{T}' = &-2\varrho_0 I_3^{-1/2}(\partial\psi/\partial\beta_1)[\mathbf{B}_e'^{-1} - (\mathbf{B}_e'^{-1} \cdot \mathbf{I}/3)\mathbf{I}] \\ &- 4\varrho_0 I_3^{-1/2}(\partial\psi/\partial\beta_2)[\mathbf{B}_e'^{-1}\mathbf{B}_e'^{-1} - (\mathbf{B}_e'^{-1} \cdot \mathbf{B}_e'^{-1}/3)\mathbf{I}].\end{aligned} \tag{2.9}$$

The flow rule for determining plastic deformation $\mathbf{C}_p$ and the evolution equations for the hardening variables κ and $\boldsymbol{\beta}$ are taken from [17]

$$\dot{\mathbf{C}}_p = \Gamma\mathbf{A}, \tag{2.10a}$$

$$\dot{\kappa} = m_1(\varrho_0\theta\xi')(Z_1 - \kappa) - A_1(\theta)Z_1[(\kappa - Z_2)/Z_1]^{r_1}, \tag{2.10b}$$

$$\begin{aligned}\dot{\boldsymbol{\beta}} = &\, m_2(\varrho_0\theta\xi')(Z_3\mathbf{U} - \boldsymbol{\beta}) - A_2(\theta)Z_1 \\ &\times [\{\mathbf{C}_p^{-1}(\boldsymbol{\beta} - \boldsymbol{\beta}_2) \cdot (\boldsymbol{\beta} - \boldsymbol{\beta}_2)\mathbf{C}_p^{-1}\}^{1/2}/Z_1]^{r_2}\mathbf{V},\end{aligned} \tag{2.10c}$$

where

$$\mathbf{A} = [3/(\mathbf{C} \cdot \mathbf{C}_p^{-1})]\mathbf{C} - \mathbf{C}_p, \quad \mathbf{A} \cdot \mathbf{C}_p^{-1} = 0, \tag{2.11a,b}$$

$$\Gamma = \Gamma_0 \exp[-(1/2)\{ZR(I_3, \theta)/\sigma_e\}^{2n(I_3, \theta)}], \tag{2.11c}$$

$$\sigma_e^2 = 3J_2 = (3/2)\mathbf{T}' \cdot \mathbf{T}' = (3/2)I_3^{-1}(\mathbf{C}\mathbf{S}' \cdot \mathbf{S}'\mathbf{C}), \tag{2.11d}$$

$$Z = \kappa + \beta, \quad \beta = \mathbf{C}_p^{-1}\boldsymbol{\beta} \cdot \mathbf{U}\mathbf{C}_p^{-1}, \tag{2.11e,f}$$

$$\mathbf{U} = \mathbf{A}/(\mathbf{C}_p^{-1}\mathbf{A} \cdot \mathbf{A}\mathbf{C}_p^{-1})^{1/2}, \tag{2.11g}$$

$$\mathbf{V} = (\boldsymbol{\beta} - \boldsymbol{\beta}_2)/\{\mathbf{C}_p^{-1}(\boldsymbol{\beta} - \boldsymbol{\beta}_2) \cdot (\boldsymbol{\beta} - \boldsymbol{\beta}_2)\mathbf{C}_p^{-1}\}^{1/2}. \tag{2.11h}$$

In (2.10) and (2.11): the function Γ causes yield-like behavior in that is nearly vanishes for low values of the effective stress σ_e and becomes significant when σ_e attains values on the order of ZR; Γ_0 is a positive constant; n is a positive function controlling strain-rate sensitivity; R is a nonnegative function which directly influences the level of flow stress; Z is a scalar measure of hardening; κ is a measure of isotropic hardening; Z_1 is the saturated value of κ; Z_2 is the fully annealed value of κ; $\boldsymbol{\beta}$ is a second order tensor measure of directional hardening; β is a scalar measure of the effect of directional hardening; Z_3 is the saturated value of β; $\boldsymbol{\beta}_2$ is the fully annealed value of $\boldsymbol{\beta}$; m_1 and m_2 are constants controlling the rate of hardening; the rate of thermal recovery is controlled by the constants r_1 and r_2, and the functions A_1 and A_2; the expression $\varrho_0\theta\xi'$ in (2.7g) and (2.10b,c) is a measure of the rate of plastic dissipation; and the condition (2.11b) ensures the plastic deformation is incompressible. Furthermore, we note that the directional hardening variable $\boldsymbol{\beta}$ was introduced by Bodner [8] to model the Bauschinger effect and it is an alternative to kinematic hardening.

3. Formulation of the numerical procedure

From (2.10a), (2.11a) and the form of Γ in (2.11c) it is obvious that the flow rule for plastic deformation rate is a highly nonlinear function of the value of effective stress σ_e. For low values of n the material response is quite rate sensitive, whereas for large values of n the material response is quite rate insensitive. Also, in this rate-insensitive limit the flow rule becomes an extremely stiff system of differential equations. For example, during loading, if the plastic deformation rate is underestimated during one time step then the prediction of the stress at the end of the time step is too large so the plastic deformation rate during the consecutive time step may be grossly overestimated causing a wild oscillation of stress.

To overcome these problems with instability of the integration procedure we assume a fully implicit scheme over a typical time interval $[t_1, t_2]$. Specifically, we determine an estimate $\bar{\mathbf{C}}_p(t_2)$ of the plastic deformation at time t_2 by the formula

$$\bar{\mathbf{C}}_p(t_2) - \mathbf{C}_p(t_1) = \Delta t \dot{\mathbf{C}}_p(t_2), \qquad \Delta t = t_2 - t_1. \tag{3.1a,b}$$

Since the flow rule (2.10a) requires plastic deformation to be incompressible (see 2.4a) the plastic deformation $\mathbf{C}_p(t_2)$ at the end of the time step is given by

$$\mathbf{C}_p(t_2) = \mathbf{C}_p'(t_2) = [\det \bar{\mathbf{C}}_p(t_2)]^{-1/3}\bar{\mathbf{C}}_p(t_2). \tag{3.2}$$

Defining the total distortional deformation $\mathbf{C}'$ by

$$\mathbf{C}' = I_3^{-1/3}\mathbf{C}, \quad \det \mathbf{C}' = 1, \tag{3.3a,b}$$

the expression for $\mathbf{A}$ in (2.11a) evaluated at the end of the time step becomes

$$\mathbf{A}(t_2) = [3/\{\mathbf{C}'(t_2) \cdot \mathbf{C}_p^{-1}(t_2)\}]\mathbf{C}'(t_2) - \mathbf{C}_p(t_2), \tag{3.4a}$$

$$\mathbf{A}(t_2) = [3/\{\mathbf{C}_e'(t_2) \cdot \mathbf{I}\}]\mathbf{C}'(t_2) - \mathbf{C}_p(t_2). \tag{3.4b}$$

In general, we may define the elastic distortional strain $\mathbf{E}_e'$ by

$$\mathbf{E}_e' = (1/2)(\mathbf{C}_e' - \mathbf{I}). \tag{3.5}$$

Since the determinant of the elastic distortional deformation $\mathbf{C}_e'$ equals unity it follows that

$$1 = \det \mathbf{C}_e' = 1 + 2\mathbf{E}_e' \cdot \mathbf{I} + O(\mathbf{E}_e' \cdot \mathbf{E}_e'), \tag{3.6a}$$

$$\mathbf{E}_e' \cdot \mathbf{I} = 0 + O(\mathbf{E}_e' \cdot \mathbf{E}_e'), \quad \mathbf{C}_e' \cdot \mathbf{I} = 3 + O(\mathbf{E}_e' \cdot \mathbf{E}_e'), \tag{3.6b,c}$$

$$\beta_1 = 3 + O(\mathbf{E}_e' \cdot \mathbf{E}_e'), \quad \beta_2 = 3 + O(\mathbf{E}_e' \cdot \mathbf{E}_e'), \tag{3.6d,e}$$

where $O(\mathbf{E}_e' \cdot \mathbf{E}_e')$ denotes terms of order of the magnitude of $\mathbf{E}_e'$ squared and higher. For most processes on a metal the elastic distortional strain $\mathbf{E}_e'$ remains small. Furthermore, we expect $\mathbf{C}_p(t_2)$ to remain close to $\bar{\mathbf{C}}_p(t_2)$ so $\mathbf{A}(t_2)$ in (3.4) is approximated by

$$\mathbf{A}(t_2) \approx \mathbf{C}'(t_2) - \bar{\mathbf{C}}_p(t_2). \tag{3.7}$$

From (2.10a) and (3.4a) we observe that the flow rule causes plastic deformation $\mathbf{C}_p$ to evolve in the direction of total distortional deformation $\mathbf{C}'$. Consequently, we assume that the value of $\bar{\mathbf{C}}_p(t_2)$ may be expressed in the alternative form

$$\bar{\mathbf{C}}_p(t_2) = \mathbf{C}'(t_2) - \lambda\bar{\mathbf{A}}, \quad \bar{\mathbf{A}} = \mathbf{C}'(t_2) - \mathbf{C}_p(t_1). \tag{3.8a,b}$$

Note from (3.8) that the scalar λ determines the extent to which plastic deformation has evolved in the direction of total distortional deformation. Specifically, if λ equals unity then the response is elastic, with $\bar{\mathbf{C}}_p(t_2)$ equal to $\mathbf{C}_p(t_1)$. On the other hand, if λ equals zero then $\bar{\mathbf{C}}_p(t_2)$ saturates to $\mathbf{C}'(t_2)$, with deviatoric stress relaxing to zero. It follows from (3.7) and (3.8) that

$$\bar{\mathbf{C}}_p(t_2) - \mathbf{C}_p(t_1) = (1-\lambda)\bar{\mathbf{A}}, \quad \mathbf{A}(t_2) \approx \lambda\bar{\mathbf{A}}. \tag{3.9a,b}$$

Furthermore, from (2.1d), (2.2c), (2.6a,b), (2.9), (3.8) and (3.9b) it can be shown that

$$\mathbf{T}'(\mathbf{F}(t_2), \bar{\mathbf{C}}_p(t_2), \theta(t_2)) = -\lambda 2\varrho_0 I_3^{-1/2}[(\partial\psi/\partial\beta_1) + 4(\partial\psi/\partial\beta_2)] \times [\bar{\mathbf{B}}_e'^{-1} - (\bar{\mathbf{B}}_e'^{-1} \cdot \mathbf{I}/3)\mathbf{I}] + O(\bar{\mathbf{A}} \cdot \bar{\mathbf{A}}) \tag{3.10a}$$

$$\bar{\mathbf{B}}_e'^{-1} = [\mathbf{F}'(t_2)^T]^{-1}\mathbf{C}_p(t_1)[\mathbf{F}'(t_2)]^{-1}, \quad \mathbf{F}' = I_3^{-1/6}\mathbf{F}, \tag{3.10b,c}$$

where the derivatives of ψ with respect to β_1, β_2 are evaluated with

$$I_3 = I_3(t_2), \quad \beta_1 = \beta_2 = 3, \quad \theta = \theta(t_2). \tag{3.11a,b,c}$$

Assuming that elastic distortional strain remains small, we neglect quadratic terms in $\bar{\mathbf{A}}$ and approximate the effective stress σ_e at the end of the time step by

$$\sigma_e[\mathbf{C}(t_2), \mathbf{C}_p(t_2), \theta(t_2)] \approx \lambda \bar{\sigma}_e, \tag{3.12a}$$

$$\bar{\sigma}_e = \sigma_e[\mathbf{C}(t_2), \mathbf{C}_p(t_1), \theta(t_2)], \tag{3.12b}$$

where $\bar{\sigma}_e$ is the effective stress that is calculated using the constitutive equation assuming that the response is elastic. In this regard, we note that it is not necessary to use the approximation (3.10a).

In view of the results (3.9a,b), (3.12a) and the expression (2.10a), it follows that the approximation (3.1a) of the flow rule reduces to a scalar equation for λ of the form

$$(1 - \lambda) = \lambda \Delta t \Gamma = \lambda \, \Delta t \Gamma_0 \exp[-(1/2)(ZR/\lambda \bar{\sigma}_e)^{2n}]. \tag{3.13}$$

During a typical process the evolution of the hardening quantity Z is quite well behaved. Consequently, for simplicity we approximate Z by its value at the beginning of the time step and specify Z, R, n in (3.13) by

$$Z = Z(t_1), \quad R = R[I_3(t_2), \theta(t_2)], \quad n = n[I_3(t_2), \theta(t_2)]. \tag{3.14a,b,c}$$

In solving (3.13) for the value of λ we may remove the stiffness in the equation by inverting the exponential function and write

$$f(\lambda) = \lambda - (ZR/\bar{\sigma}_e)[2 \ln\{\Delta t \Gamma_0 \lambda/(1 - \lambda)\}]^{-(1/2n)}, \tag{3.15}$$

where the solution of (3.13) is the root of the function $f(\lambda)$ in (3.15). However, if the material melts and R vanishes (see [12]) then it is more convenient to solve (3.13) directly to obtain

$$\lambda = 1/(1 + \Delta t \Gamma_0). \tag{3.16}$$

In any case, it is easy to see that

$$f(\lambda_{\min}) = \lambda_{\min} - 1 < 0 < f(1) = 1, \tag{3.17}$$

so the solution of (3.15) lies in the range

$$\lambda_{\min} \leq \lambda < 1, \tag{3.18}$$

where the values of $\lambda_{\min}$ is determined by requiring the second term on the right hand side of (3.15) to equal unity

$$\lambda_{\min} = 1/[1 + \Delta t \Gamma_0 \exp\{-(1/2)(ZR/\bar{\sigma}_e)^{2n}\}]. \tag{3.19}$$

Notice, that if R vanishes then the value of $\lambda_{\min}$ reduces to the solution (3.16). Furthermore, by differentiating $f(\lambda)$ with respect to λ it can be shown that f is a monotonically increasing function of λ in the range (3.18). Consequently, f has only a single root in this range. For the examples discussed in this paper the root of (3.15) was determined using the simple secant method. It was found that this method works quite well even when the material response is nearly rate insensitive (with n being very large) and/or large time steps are taken.

In summary, we assume that the values of all quantities are known at the beginning of the time step ($t = t_1$) and that the total deformation $\mathbf{C}$ and temperature θ are known at the end of the time step ($t = t_2$). If R is positive, the value of λ is determined by numerically solving for the root of $f(\lambda)$ in (3.15) with the specifications (3.12b) and (3.14). Otherwise, if R vanishes, then the value of λ becomes (3.16). Once λ is determined, the value of plastic deformation $\mathbf{C}_p(t_2)$ at the end of the time step is determined using (3.2) and (3.8). The values of the isotropic hardening κ and directional hardening $\boldsymbol{\beta}$ may be updated by numerically integrating equations (2.10b,c) using an average value of $\dot{\mathbf{C}}_p$ in (2.7g). Specifically, in the absence of thermal recovery ($A_1 = A_2 = 0$), we assume that the rate of plastic dissipation $\varrho_0 \theta \xi'$ remains reasonably constant during the time interval and approximate the integrals of (2.10b,c) by

$$\kappa(t_2) = Z_1 - [Z_1 - \kappa(t_1)] \exp(-m_1 \varrho_0 \theta \xi' \Delta t), \tag{3.20a}$$

$$\boldsymbol{\beta}(t_2) = Z_3 \mathbf{U} - [Z_3 \mathbf{U} - \boldsymbol{\beta}(t_1)] \exp(-m_2 \varrho_0 \theta \xi' \Delta t), \tag{3.20b}$$

$$\varrho_0 \theta \xi' \Delta t \approx (1/2) \mathbf{C}_p^{-1} \mathbf{C} \mathbf{S}' \cdot [\mathbf{C}_p(t_2) - \mathbf{C}_p(t_1)], \tag{3.20c}$$

where $\mathbf{C}$, $\mathbf{C}_\mathrm{p}$, $\mathbf{S}'$, $\mathbf{U}$ are evaluated at the end of the time step ($t = t_2$).

4. Compression-shear

Compression-shear is a deformation associated with modern tests used to determine dynamic plastic properties of materials [27]. This deformation is considered here as an example for three reasons: first, total deformation is specified so there is no need to solve boundary conditions by iteration (see the example of simple tension in the next section); second, large deformation simple shear can be analyzed as a special case; and third, a corner test representing a transition from compression to shear can be used to examine the accuracy of the numerical procedure for abrupt changes in the direction of loading.

Throughout the text all tensor quantities are referred to a fixed rectangular Cartesian coordinate system with base vectors $\mathbf{e}_i$ ($i = 1, 2, 3$). Specifically let X_A ($A = 1, 2, 3$) and x_i be the components of $\mathbf{X}$, and $\mathbf{x}$, respectively. Then, by considering compression in the $\mathbf{e}_1$ direction and shear in the $\mathbf{e}_2$

direction, we specify

$$x_1 = a(t)X_1, \quad x_2 = \gamma(t)X_1 + X_2, \quad x_3 = X_3, \tag{4.1a,b,c}$$

where $a(t)$ controls the amount of compression and $\gamma(t)$ controls the amount of shear. It follows that for this deformation

$$\mathbb{F} = \begin{pmatrix} a & 0 & 0 \\ \gamma & 1 & 0 \\ 0 & 0 & 1 \end{pmatrix}, \quad \mathbb{F}^{-1} = a^{-1}\begin{pmatrix} 1 & 0 & 0 \\ -\gamma & a & 0 \\ 0 & 0 & a \end{pmatrix}, \tag{4.2a,b}$$

$$\mathbb{C} = \begin{pmatrix} a^2+\gamma^2 & \gamma & 0 \\ \gamma & 1 & 0 \\ 0 & 0 & 1 \end{pmatrix}, \quad \mathbb{C}^{-1} = a^{-2}\begin{pmatrix} 1 & -\gamma & 0 \\ -\gamma & a^2+\gamma^2 & 0 \\ 0 & 0 & a^2 \end{pmatrix}, \tag{4.2c,d}$$

$$I_3 = a^2 \tag{4.2e}$$

To test the numerical procedure proposed in the last section we consider the purely mechanical theory and specify the Helmholtz free energy ψ in the form

$$2\varrho_0\psi = k_0[6(I_3^{-1/6} - 1) + 3(I_3^{1/3} - 1)] + \mu_0(\beta_1 - 3), \tag{4.3}$$

where the bulk modulus k_0 and the shear modulus μ_0 may be determined by considering standard elastic tests in the small deformation range. Using (2.7b) the pressure becomes

$$p = k_0[I_3^{-2/3} - I_3^{-1/6}]. \tag{4.4}$$

It will be seen in the next section that this form of the pressure simplifies the determination of the lateral stretch in simple tension.

Using the procedure described in the last section, a computer program was developed to calculate the stress response to compression-shear for constant rate $\dot{a}$ and constant shear rate $\dot{\gamma}$. The variables a and γ were specified by

$$da/dt = \dot{a}, \quad a(0) = 1, \quad d\gamma/dt = \dot{\gamma}, \quad \gamma(0) = 0 \tag{4.5a,b,c,d}$$

where $\dot{a}$, $\dot{\gamma}$ are constant during time intervals and $\dot{a}$ jumps from a constant nonzero value to zero and $\dot{\gamma}$ jumps from zero to a constant nonzero value at the transition from compression to shear.

As a first test of the computer program we attempted to recalculate the results presented in [12] for simple shear ($\dot{a} = 0, a = 1$) which used an integration procedure of the type proposed by Kanchi *et al.* [13]. Consequently, for the calculations presented in this paper we specify

$$k_0 = 78.0 \text{ GPa}, \quad \mu_0 = 44.0 \text{ GPa}, \tag{4.6a,b}$$

$$\Gamma_0 = 10^8 \text{ s}^{-1}, \quad R = 1.0, \tag{4.6c, d}$$

$$m_1 = 100(\text{GPa})^{-1}, \quad m_2 = 4000(\text{GPa})^{-1}, \tag{4.6e,f}$$

$$A_1 = A_2 = 0. \tag{4.6g}$$

The initial values of plastic deformation $\mathbf{C}_p$, isotropic hardening κ and directional hardening $\boldsymbol{\beta}$ are taken as

$$\mathbf{C}_p = \mathbf{I}, \quad \kappa = \kappa_0, \quad \boldsymbol{\beta} = 0. \tag{4.7a,b,c}$$

Also, depending on the problem we specify κ_0, Z_1 and Z_3 by

$$n = 1.0, \quad \kappa_0 = 3.0 \text{ GPa}, \quad Z_1 = 3.0 \text{ GPa}, \quad Z_3 = 0 \text{ GPa}, \tag{4.8a}$$

$$n = 100.0, \quad \kappa_0 = Z_1, \quad Z_1 = 0.456 \text{ GPa}, \quad Z_3 = 0 \text{ GPa}, \tag{4.8b}$$

$$n = 1.0, \quad \kappa_0 = 1.7 \text{ GPa}, \quad Z_1 = 2.0 \text{ GPa}, \quad Z_3 = 1.0 \text{ GPa}. \tag{4.8c}$$

Analyzing the results of the calculation for simple shear we observed again that once the hardening variables saturated the components T_{ij} of the Cauchy stress $\mathbf{T}$ saturated to constant values. Furthermore, it was observed that the component C_{p22} $(= C_{p33})$ of the plastic deformation $\mathbf{C}_p$ also saturated to a constant value. These results suggest that it may be possible to obtain an analytical solution which is asymptotically valid in the region where the hardening variables have saturated and the stress has become constant. Indeed, this is the case. Specifically, we show that in this region the flow rule (2.10a) becomes

$$\dot{C}_{p11} = \Gamma[c(1 + \gamma^2) - C_{p11}], \quad c = 3/(\mathbf{C} \cdot \mathbf{C}_p^{-1}), \tag{4.9a,b}$$

$$\dot{C}_{p22} = \Gamma[c - C_{p22}], \quad \dot{C}_{p33} = \dot{C}_{p22}, \tag{4.9c,d}$$

$$\dot{C}_{p12} = \Gamma[c\gamma - C_{p12}], \quad \dot{C}_{p13} = \dot{C}_{p23} = 0, \tag{4.9e,f}$$

where Γ and c attain constant values. Since these equations are linear and γ is specified by (4.5b) they may be easily integrated. As an example, equation (4.9c) yields

$$C_{p22}(t) = c + [C_{p22}(t_1) - c] \exp[-(\Gamma/\dot{\gamma})(\gamma - \gamma_1)], \tag{4.10}$$

where γ_1 is the value of γ at $t = t_1$. It follows that for large values of γ the exponential term in (4.10) is negligible which demonstrates that the material tends to forget certain features of its reference configuration. Similarly, it may be shown that for large values of γ we may obtain the asymptotic solution

$$C_{p11}(t) \to c[1 + \gamma^2 - (2\dot{\gamma}/\Gamma)(\gamma - \dot{\gamma}/\Gamma)], \tag{4.11a}$$

$$C_{p22}(t) = C_{p33}(t) \to c, \tag{4.11b}$$

$$C_{p12}(t) \to c[\gamma - (\dot{\gamma}/\Gamma)]. \tag{4.11c}$$

However, since we are requiring plastic deformation to be incompressible, the value of c may be determined by the condition (2.4a) to obtain

$$c = [1 + (\dot{\gamma}/\Gamma)^2]^{-1/3}. \tag{4.12}$$

Using these asymptotic results it may be shown that $\mathbf{B}_e$ also becomes a constant tensor such that

$$\mathbf{B}_e^{-1} \to [1 + (\dot{\gamma}/\Gamma)^2]^{-1/3} \begin{pmatrix} 1 + 2(\dot{\gamma}/\Gamma)^2 & -(\dot{\gamma}/\Gamma) & 0 \\ -(\dot{\gamma}/\Gamma) & 1 & 0 \\ 0 & 0 & 1 \end{pmatrix}. \tag{4.13}$$

It follows from (2.5a), (2.6a,b) and (2.9) that since $\mathbf{B}_e$ is constant the quantities β_1, β_2 are also constant so the Cauchy stress $\mathbf{T}$ becomes a constant tensor for simple shear at constant shearing rate and constant temperature even if the Helmholtz free energy ψ is a general function of its arguments. In other words, the exact asymptotic solution (4.11)–(4.13) is valid for an arbitrary material in the class defined by (2.5a).

Once the form of ψ is specified, equation (2.9) may be used to determine the Cauchy stress $\mathbf{T}$ and the effective stress σ_e may be determined from (2.11d) as a function of the constant value of Γ. Substituting the result into (2.11c) and using the saturated value of Z, we obtain an equation which may be solved numerically to find the appropriate value of the constant Γ for the specified shearing rate $\dot{\gamma}$.

For the specific material defined by (4.3) the components T_{ij} of Cauchy stress associated with the asymptotic solution become

$$T_{11} = -\mu_0[1 + (\dot{\gamma}/\Gamma)^2]^{-1/3}[(4/3)(\dot{\gamma}/\Gamma)^2], \tag{4.14a}$$

$$T_{22} = T_{33} = -T_{11}/2, \tag{4.14b}$$

$$T_{12} = \mu_0[1 + (\dot{\gamma}/\Gamma)^2]^{-1/3}(\dot{\gamma}/\Gamma), \tag{4.14c}$$

$$T_{13} = T_{33} = 0. \tag{4.14d}$$

Using the integration procedure described in section 3 we calculated the response to simple shear and compression-shear. Figures 1–3 examine the response for a constant value of the hardening Z. Figures 1a and 1b show the results for simple shear of the rate sensitive material characterized by (4.8a) using different step sizes $\Delta\gamma$. The values of T_{12} and T_{22} correspond to a final value of $\gamma = 0.1$ and two constant shear rates, which differ by eight orders of magnitude, have been considered. Notice that for both rates the shear stress T_{12} is quite accurate even for a single step $\Delta\gamma = 0.1$, which corresponds to nearly 130 times the value of γ at yield for the lower rate. The value of shear stress for the higher rate is slightly low because the numerical procedure uses the average plastic deformation rate and the rate sensitivity of the material increases with increase in plastic deformation rate

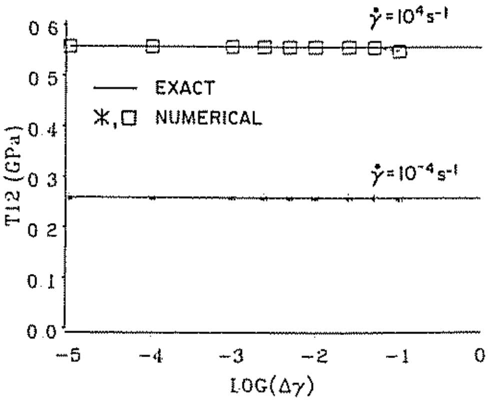

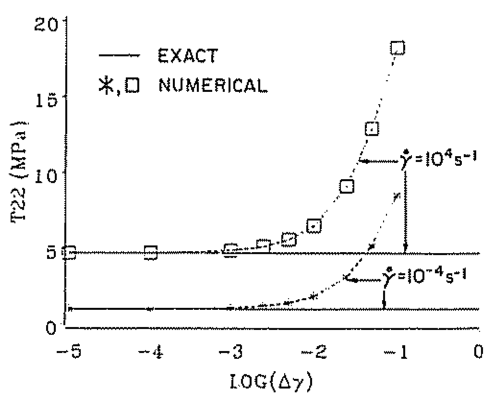

Figure 1a
Simple Shear: Values of the shear stress calculated for the rate sensitive material characterized by (4.8a) and a final value of $\gamma = 0.1$. The influence of changing the step size $\Delta\gamma$ and the shearing rate $\dot{\gamma}$ is shown.

Figure 1b
Simple Shear: Values of the normal stress calculated for the rate sensitive material characterized by (4.8a) and a final value of $\gamma = 0.1$. The influence of changing the step size $\Delta\gamma$ and the shearing rate $\dot{\gamma}$ is shown.

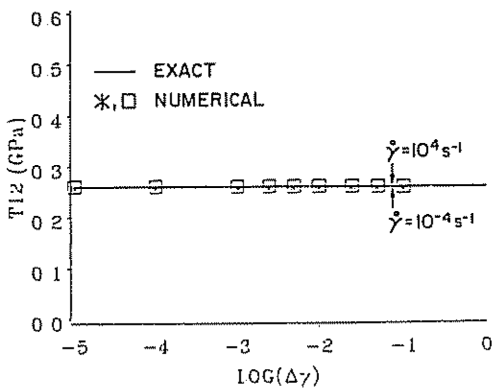

Figure 2
Simple Shear: Values of the shear stress calculated for the rate insensitive material characterized by (4.8b) and a final value of $\gamma = 0.1$. The influence of changing the step size $\Delta\gamma$ and the shearing rate $\dot{\gamma}$ is shown.

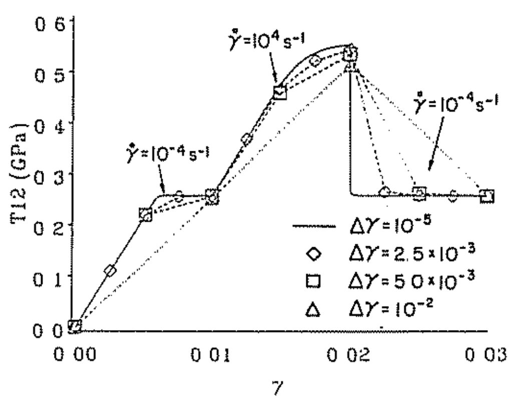

Figure 3
Simple Shear: Values of the shear stress calculated for the material characterized by (4.8a) and a jump test between the rates $\dot{\gamma} = 10^{-4}\,s^{-1}$ and $\dot{\gamma} = 10^{4}\,s^{-1}$. The influence of changing the step size $\Delta\gamma$ is shown.

(see [9] Fig. 1). Notice also that the error in the calculation of the normal stress T_{22} increases with increased step size. However, in all cases the normal stresses are nearly two orders of magnitude lower than the shear stress. Furthermore, we note that the exact asymptotic results in Fig. 1 for the lower rate are identical to the saturated values presented in [12] once we observe that the values of T_{11}, T_{22} in this paper correspond to T_{22}, T_{11}, respectively, in [12].

Figure 2 shows the results for simple shear of the nearly rate insensitive material characterized by (4.8b) using different step sizes $\Delta\gamma$. The values of T_{12} correspond to a final value of $\gamma = 0.1$ and two constant shear rates have been considered. The value of Z_1 in (4.8b) was chosen to produce a value of effective stress σ_e for the low rate $\dot{\gamma} = 10^{-4}\ \mathrm{s}^{-1}$ equal to that associated with the material (4.8a). Specifically, the value $Z(n)$ of the hardening variable Z associated with a material with rate sensitivity parameter n may be determined to produce the same value of σ_e for material (4.8a) shearing at the rate $\dot{\gamma} = 10^{-4}\ \mathrm{s}^{-1}$ by requiring the argument of the exponential function in (2.11c) to remain constant. Thus, for our case we have

$$Z(n) = \sigma_e(n_1)[Z(n_1)/\sigma_e(n_1)]^{n_1/n}, \tag{4.15a}$$

$$n_1 = 1, \quad Z(1) = 3.0\ \mathrm{GPa}, \quad \sigma_e(1) = 0.447\ \mathrm{GPa}, \tag{4.15b,c,d}$$

where R has been taken to be unity.

Notice from Fig. 2 that the material response is quite rate insensitive because the differences in the curves are insignificant even when the shearing rate is changed by eight orders of magnitude. By comparing Fig. 2 with Fig. 1a we observe that the prediction of the shear stress for $\Delta\gamma = 0.1$ is more accurate for the nearly rate insensitive material than for the rate sensitive material. Further, the results for the normal stress T_{22} have not been presented because both the curves for low and high rates are nearly identical to the one presented in Fig. 1b for $\dot{\gamma} = 10^{-4}\ \mathrm{s}^{-1}$.

Figure 3 shows the results for simple shear of the rate sensitive material characterized by (4.8a) using different step sizes $\Delta\gamma$. This figure shows the ability of the procedure to calculate a jump test specified by

$$\dot{\gamma} = 10^{-4}\ \mathrm{s}^{-1} \quad \text{for } (0 \le \gamma < 0.01), \tag{4.16a}$$

$$\dot{\gamma} = 10^{4}\ \mathrm{s}^{-1} \quad \text{for } (0.01 \le \gamma < 0.02), \tag{4.16b}$$

$$\dot{\gamma} = 10^{-4}\ \mathrm{s}^{-1} \quad \text{for } (0.02 \le \gamma \le 0.03). \tag{4.16c}$$

Notice that the results are good even when $\Delta\gamma = 10^{-2}$ and there is only one point calculated for each of the shear rates. Specifically, the stress faithfully follows the increase and decrease in shear rate. Again we note that the values predicted for the higher rate are slightly low because the rate sensitivity is increased at the higher rate.

Figure 4 shows the results for simple shear of the rate sensitive material

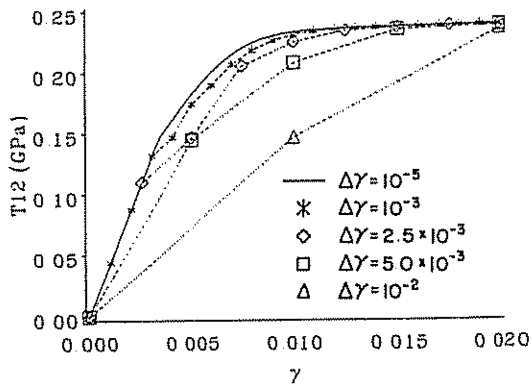

Figure 4
Simple Shear: Values of the shear stress calculated for the hardening material characterized by (4.8c). The influence of changing the step size $\Delta\gamma$ is shown for the shearing rate $\dot{\gamma} = 10^{-4}\,s^{-1}$.

characterized by (4.8c) using different step sizes $\Delta\gamma$ and a rate $\dot{\gamma} = 10^{-4}\,s^{-1}$. Most of the hardening exhibited in this figure is due to directional hardening. Recall that the numerical procedure updates the value of hardening Z only after calculating plasticity based on the initial value of Z. Consequently, the curves show a delay in the effect of hardening. However, it is important to note that although the value of stress for the curve $\Delta\gamma = 10^{-2}$ is underpredicted for $\gamma = 0.01$ the value of stress is relatively accurate for $\gamma = 0.02$. This is because the initial value of Z for the second step incorporated the fact that the directional hardening β nearly saturated during the first step.

Figures 5a and 5b show the results for compression followed by shear of the rate sensitive material characterized by (4.8c). During the compression $\dot{a} = -10^{-4}\,s^{-1}$ and during the shear $\dot{\gamma} = 10^{-4}\,s^{-1}$. For convenience the results are presented in terms of the average strain E_{avg} defined by

$$E_{avg} = |1 - a| + |\gamma|, \tag{4.17}$$

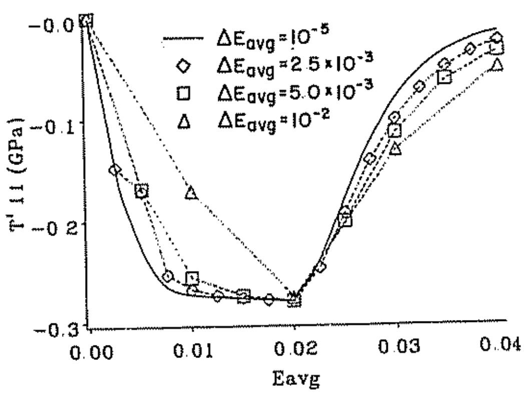

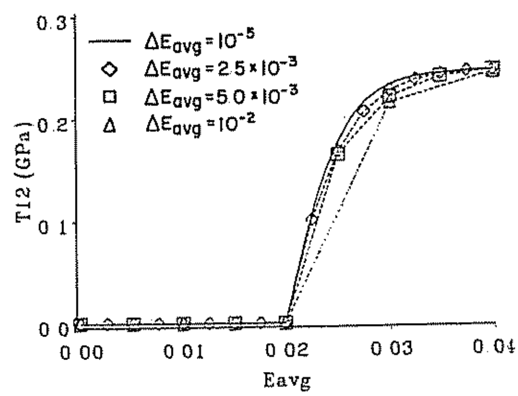

Figure 5a
Compression-Shear: Values of the deviatoric stress calculated for the hardening material characterized by (4.8c). The influence of changing the step ΔE_{avg} is shown for the compression rate $\dot{a} = -10^{-4}\,s^{-1}$ and the shearing rate $\dot{\gamma} = 10^{-4}\,s^{-1}$.

Figure 5b
Compression-Shear: Values of the shear stress calculated for the hardening material characterized by (4.8c). The influence of changing the step ΔE_{agv} is shown for the compression rate $\dot{a} = -10^{-4}\,s^{-1}$ and the shearing rate $\dot{\gamma} = 10^{-4}\,s^{-1}$.

using different step sizes ΔE_{avg}. In general, the results faithfully follow the trend that the deviatoric stress T'_{11}, decreases and the shear stress T_{12} increases to the values associated with simple shear (Fig. 1, eqn. (4.14)) as the shear is being applied. The errors shown in Fig. 5a for the compression phase are mainly due to the delay in the effect of hardening whereas the errors in the shearing phase are mainly due to the inability of a single parameter scheme to accurately follow the evolution of each of the components of plastic deformation $\mathbf{C}_p$ when $\mathbf{C}_p$ is changing directions. In this latter regard, the errors in the shearing phase are similar to those which have been analyzed by Krieg and Krieg [28] for small deformations using a yield function and the radial return method [14]. Furthermore, we emphasize the value of T_{11} is obtained by superimposing a value of pressure which increases nearly linearly from zero to 1.60 GPa during the compression phase. Thus, the errors in T'_{11} become insignificant relative to the value of T_{11}.

5. Simple tension

Although simple tension is one of the easiest experiments to perform, complications arise in its analysis because it is necessary to satisfy the boundary condition of zero lateral stress. This influences the implementation of the solution procedure described in section 3 because the lateral stretch is not known at the end of the time step even if axial stretch is imposed.

The deformation quantities for simple tension may be written in the form

$$x_1 = a(t)X_1, \quad x_2 = b(t)X_2, \quad x_3 = b(t)X_3, \tag{5.1a,b,c}$$

$$F_{11} = a, \quad F_{22} = F_{33} = b, \quad \text{all other } F_{iA} = 0, \tag{5.1d,e,f}$$

$$C_{11} = a^2, \quad C_{22} = C_{33} = b^2, \quad \text{all other } C_{AB} = 0, \tag{5.1g,h,i}$$

$$I_3 = a^2 b^4, \tag{5.1j}$$

where $a(t)$ is the axial stretch and $b(t)$ is the lateral stretch. Also, F_{iA} and C_{AB} are the components of $\mathbf{F}$ and $\mathbf{C}$, respectively. Using the flow rule (2.10a), (2.11a) and imposing plastic incompressibility the components of plastic deformation become

$$C_{p11} = a_p^2, \quad C_{p22} = C_{p33} = 1/a_p, \quad \text{all other } C_{pAB} = 0, \tag{5.2a,b,c}$$

where the value of a_p is to be determined.

It follows that for the specification (4.3) the components T'_{ij} of the deviatoric Cauchy stress $\mathbf{T}'$ become

$$T'_{11} = \mu_0(2I_3^{-2/3}/3aa_p)(a^2 - a_p^3 b^2), \tag{5.3a}$$

$$T'_{22} = T'_{33} = -T'_{11}/2, \quad \text{all other } T'_{ij} = 0. \tag{5.3b,c}$$

Now, the value of the lateral stretch b may be determined by requiring the lateral stress T_{22} to vanish

$$T_{22} = -p + T'_{22} = 0. \tag{5.4}$$

Substituting (4.4) and (5.3) into (5.4) and multiplying the result by $I_3^{2/3}$ we obtain

$$k_0(1 - I_3^{1/2}) + (\mu_0/3aa_p)(a^2 - a_p^3 b^2) = 0. \tag{5.5}$$

Since $I_3^{1/2}$ is a linear function of b^2 (5.1j) it follows that (5.5) admits the simple solution

$$b^2 = (1/a)[1 + (\mu_0/3k_0)(a/a_p)]/[1 + (\mu_0/3k_0)(a_p/a)^2]. \tag{5.6}$$

Other nonlinear forms for the pressure, different from (4.4), could be postulated which would also yield a simple expression for the lateral stretch. However, since the volume change for a metal should remain quite small for simple tension and since all of these forms must yield the same linearized expression for pressure, any differences that arise should remain insignificant.

Now, to solve the problem of simple tension we first specify the axial stretch $a(t)$; then guess a value of b at the end of the time step; calculate a_p using the procedure of section 3; and finally iterate on the guess for b until equation (5.6) is satisfied at the end of the time step.

Figure 6a shows the calculation of simple extension for the rate sensitive material characterized by (4.8a), a constant rate $\dot{a} = 10^{-4}\,\mathrm{s}^{-1}$, and three step sizes Δa. Notice that the solution is quite accurate even for an extremely large step size $\Delta a = 9$ (which is three orders of magnitude larger than the value of Δa associated with yield). Figure 6b shows the calculation of simple

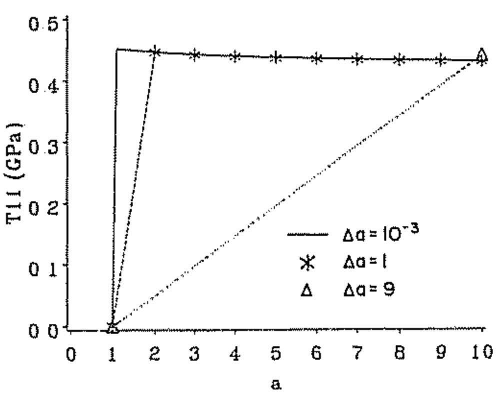

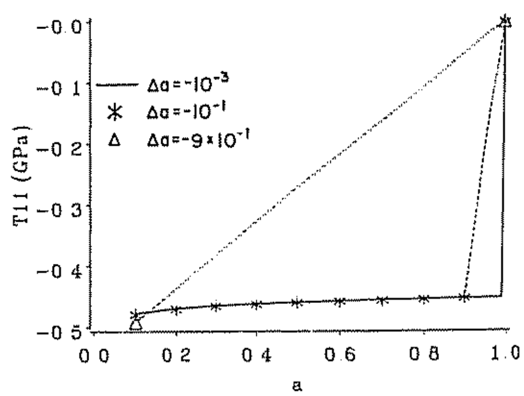

Figure 6a
Simple Tension: Values of the stress for extension at constant rate $\dot{a} = 10^{-4}\,\mathrm{s}^{-1}$ of the rate sensitive material characterized by (4.8a). The influence of changing the step Δa is shown.

Figure 6b
Simple Tension: Values of the stress for contraction at constant rate $\dot{a} = -10^{-4}\,\mathrm{s}^{-1}$ of the rate sensitive material characterized by (4.8a). The influence of changing the step Δa is shown.

compression for the same rate sensitive material, a constant rate $\dot{a} = -10^{-1}\,\mathrm{s}^{-1}$, and three step sizes Δa. Notice that the solution is quite accurate even for $\Delta a = -0.9$.

6. Application to other models

The numerical procedure of section 3 was developed with specific reference to a generalized version of the elastic-viscoplastic model proposed by Bodner and Partom [6, 7] which does not use a yield function. Here, we show that the same procedure may be used for other models of plastic behavior. Specifically, we consider a rate-insensitive model which uses the notion of a yield surface as well as a form of the overstress model for rate-sensitive response.

To this end, let g be a yield function in strain space [29] which separates elastic and plastic response. Constitutive equations of the type discussed in this paper may be reformulated using a yield function by modifying the function Γ in (2.10a) and neglecting thermal recovery of hardening ($A_1 = A_2 = 0$ in (2.10b,c)). A detailed discussion of the formulation for anisotropic materials may be found in [16]. For our present purpose we consider a simple yield function specified by

$$g = g(\mathbf{C}, \mathbf{C}_p, \theta, \kappa, \boldsymbol{\beta}) = 1 - (ZR/\sigma_e)^2. \tag{6.1}$$

For this model, loading into the plastic region is characterized by

$$g = 0 \quad \text{and} \quad \hat{g} = (\partial g/\partial \mathbf{C}) \cdot \dot{\mathbf{C}} + (\partial g/\partial \theta)\dot{\theta} > 0, \tag{6.2}$$

and elastic response is characterized by

$$g = 0 \quad \text{and} \quad \hat{g} \le 0, \quad \text{or} \quad g < 0. \tag{6.3a,b}$$

The quantity $\hat{g}$ in (6.2) indicates loading by evaluating the tendency for the yield function to increase due to elastic response only.

In the present context, the expression (3.12a) for the effective stress σ_e may be used to rewrite (6.1) in the form

$$g = 1 - (ZR/\lambda\bar{\sigma}_e)^2. \tag{6.4}$$

Consequently, loading into the plastic region and elastic response may be approximated by

$$\lambda = (ZR/\bar{\sigma}_e) \quad \text{for loading } (\bar{\sigma}_e > ZR), \tag{6.5a}$$

$$\lambda = 1 \quad \text{for elastic response } (\bar{\sigma}_e \le ZR). \tag{6.5b}$$

The value of λ in (6.5a) is determined by the consistency condition which requires the yield function g to vanish at the end of the time step. Since $\bar{\sigma}_e$ is evaluated assuming only elastic response during the time step, the condition that $\bar{\sigma}_e$ is greater than ZR indicates that elastic response tends to increase the value of the yield function. Consequently, the condition (6.5a) is compatible with the loading condition (6.2). A detailed discussion of the compatibility of numerical procedures and the strain-space formulation of plasticity has been given by Moss [30]. Furthermore, we note that for the small deformation theory the equations of section 3 together with the specification (6.5a) reduce to the radial return method [14].

In calculating the value of plastic deformation at the end of the time step we assume that Z and R in (6.5) attain the values (3.14a,b). Therefore, the value of Z must be updated after plastic deformation has been calculated.

A form of the overstress model [2, 3] may be obtained by assuming the function Γ in (2.10a), (2.11c) is replaced by

$$\Gamma = \Gamma_0 g^m \quad \text{for loading } (g > 0), \tag{6.6a}$$

$$\Gamma = 0, \lambda = 1 \quad \text{for elastic response } (g \leq 0), \tag{6.6b}$$

where Γ_0 and m are positive constants controlling the rate-sensitivity of the response and g is the yield function given by (6.1) and (6.4). In this formulation the consistency condition is abandoned and the yield function g is allowed to become positive. Furthermore, plastic deformation rate experiences a continuous transition from elastic to plastic response because it vanishes when g vanishes. In constrast, the consistency condition in the rate-insensitive model forces plastic deformation rate to experience a jump when the material begins to yield.

Using the procedure described in section 3 and replacing the function Γ in (3.13) with the expression (6.6a) we obtain

$$(1 - \lambda) = \lambda\, \Delta t \Gamma_0 [1 - [(ZR/\lambda \bar{\sigma}_e)^2]^m, \tag{6.7}$$

which is an equation to determine λ during loading. Rearranging (6.7), the analogue of the function $f(\lambda)$ in (3.15) becomes

$$f(\lambda) = \lambda - (ZR/\bar{\sigma}_e)[1 - \{(1 - \lambda)/\lambda\, \Delta t \Gamma_0\}^{1/m}]^{-1/2}. \tag{6.8}$$

With the help of the definition

$$\lambda_{\min} = 1/(1 + \Delta t \Gamma_0), \tag{6.9}$$

it is easy to show that

$$f(\lambda_{\min}) = -\infty < 0 < f(1) = 1 - (ZR/\bar{\sigma}_e), \tag{6.10}$$

so the root of (6.8) lies in the range

$$\lambda_{\min} < \lambda < 1. \tag{6.11}$$

Furthermore, by differentiating $f(\lambda)$ with respect to λ it can be shown that f is a monotonically increasing function of λ in the range (6.11).

Consequently, f has only a single root in this range. Notice also, that for very large values of the constant m the material response becomes quite rate-insensitive because the root of (6.8) approaches the value (6.5a). However, if thermal recovery of hardening is retained by specifying nonzero values of A_1, A_2 then a certain amount of rate sensitivity remains even if the evolution equation for plastic deformation becomes nearly rate insensitive.

Finally, we mention that for both of these models the notion of melting, as represented by a vanishing value of R, causes deviatoric stress to vanish. This result should be contrasted with the more physical result associated with the constitutive equations of section 2 which requires the metal to flow as a viscous fluid when it melts [12].

7. A modified estimate of hardening

It was seen in Figs. 4 and 5a that the numerical procedure of section 3 produces a delayed effect of hardening because the value of the hardening variable Z is only updated after plastic deformation has been calculated. Here, we consider a simple modification of the estimate of the hardening which significantly improves the results for hardening materials. Specifically, let κ^*, β^*, z^* be the values of κ, β, z at the end of the time step estimated by the procedure of section 3. Further, let ΔZ_{error} be a specified nondimensional error parameter and test if the change in Z exceeds the limit determined by

$$|Z^* - Z(t_1)|/Z^* \leq \Delta Z_{\text{error}}, \tag{7.1}$$

where we recall that $Z(t_1)$ is the value of Z at the beginning of time step.

If equation (7.1) is satisfied then the values determined by the procedure of section 3 are accepted without correction. Otherwise, $\mathbf{C}_p$, κ, $\boldsymbol{\beta}$ are reset to their values at the beginning of the time step and the values of $\mathbf{C}_p$, κ, $\boldsymbol{\beta}$ at the end of the time step are recalculated using the procedure of section 3 with Z in (3.14a) replaced by a new trial value Z_T. The value of Z_T is determined by the weighted average

$$Z_T = \kappa_T + \beta_T, \tag{7.2a}$$

$$\kappa_T = \kappa(t_1) + [\alpha_1 + (1 - \alpha_1)(\kappa^* - Z_2)/(Z_1 - Z_2)][\kappa^* - \kappa(t_1)], \tag{7.2b}$$

$$\beta_T = \beta(t_1) + [\alpha_2 + (1 - \alpha_2)|\beta^*|/Z_3][\beta^* - \beta(t_1)], \tag{7.2c}$$

$$0 \leq \alpha_1 \leq 1, \quad 0 \leq \alpha_2 \leq 1, \tag{7.2d,e}$$

where α_1 and α_2 are quantities to be determined. The trial values κ_T, β_T have the property that for any values of α_1, α_2 they incorporate the full change in the hardening variables κ, β if κ^* and $|\beta^*|$ attain their saturated values Z_1

and Z_3, respectively. Obviously, if Z_3 and $\boldsymbol{\beta}_2$ vanish then the trial value of the directional hardening parameter (7.2c) is not calculated.

In order to motivate a form for α_1 it suffices to consider the small deformation theory (see appendix), discuss the simple case of plastic deformation at constant loading rate and neglect directional hardening ($Z = \kappa$). In section 3, plastic deformation at the end of the time step was calculated using the value of hardening $\kappa(t_1)$ at the beginning of the time step. It follows that during loading the plastic work done may be approximated by

$$\mathbf{T}' \cdot \Delta\mathbf{E}_p = \mathbf{T}'^* \cdot \Delta\mathbf{E}_p^*, \tag{7.3}$$

where $\Delta\mathbf{E}_p^*$ is the plastic strain increment during the time step and $\mathbf{T}'^*$ is the estimate of deviatoric stress at the end of the time step. Neglecting thermal recovery and using Euler integration the updated value κ^* of κ obtained using (2.10b) becomes (see A10)

$$\kappa^* - \kappa(t_1) = m_1[\mathbf{T}'^* \cdot \Delta\mathbf{E}_p^*][Z_1 - \kappa(t_1)]. \tag{7.4}$$

However, if plasticity were calculated using the final value $\kappa(t_2)$ then the plastic work done would be approximated by

$$\mathbf{T}' \cdot \Delta\mathbf{E}_p = \mathbf{T}'(t_2) \cdot [\Delta\mathbf{E}_p^* - \Delta\mathbf{E}_e'] = \mathbf{T}'(t_2) \cdot [\Delta\mathbf{E}_p^* - \Delta\mathbf{T}'/2\mu_0], \tag{7.5}$$

where $\Delta\mathbf{T}'$ is the deviatoric stress increment from $\mathbf{T}'^*$ to $\mathbf{T}'(t_2)$, $\mathbf{T}'(t_2)$ is the deviatoric stress at the end of the time step, μ_0 is the reference value of the shear modulus, and (A3) has been used. Furthermore, for proportional loading at constant rate $\Delta\mathbf{T}'$ may be approximated by

$$\Delta\mathbf{T}' = [\kappa(t_2) - \kappa(t_1)]\mathbf{T}'^*/\sigma_e^*, \tag{7.6}$$

where σ_e^* is the value of effective stress associated with $\mathbf{T}'^*$. Since to first order $\mathbf{T}'(t_2)$ in (7.5) may be replaced by $\mathbf{T}'^*$ it follows that the updated value of hardening $\kappa(t_2)$ becomes

$$\kappa(t_2) - \kappa(t_1) = \alpha_1[\kappa^* - \kappa(t_1)], \tag{7.7a}$$

$$\alpha_1 = 1/[1 + m_1\{Z_1 - \kappa(t_1)\}\lambda\bar{\sigma}_e/3\mu_0], \tag{7.7b}$$

where (7.4) has been used and the value σ_e^* has been related to $\bar{\sigma}_e$ using the expression (A9a). Notice that for values of κ^* close to Z_2 the trial value κ_T in (7.2b) is the same as the final value $\kappa(t_2)$ in (7.7), which is the desired result.

For the general case when both directional and isotropic hardening are included and the loading is not necessarily proportional or at constant rate we continue to assume that the expression (7.7b) holds. Also, by analogy, we specify α_2 by

$$\alpha_2 = 1/[1 + m_2\{Z_3 - |\beta(t_1)|\}\lambda\bar{\sigma}_e/3\mu_0]. \tag{7.8}$$

The problems of simple shear and compression-shear associated with Figs. 4 and 5 were resolved using the modified estimate of hardening discussed above together with the specification

$$\Delta Z_{\text{error}} = 10^{-2}. \tag{7.9}$$

Figure 7 shows the results for simple shear. The modified method appears to predict accurate results for any step size. In particular, note that the modified solution for $\Delta\gamma = 5.0 \times 10^{-3}$ in Fig. 7 is more accurate than the solution for $\Delta\gamma = 2.5 \times 10^{-3}$ in Fig. 4. Since the computational time for the modified method associated with each step which fails the test (7.1) is less than twice that for a step which passes the test (7.1) it might be more efficient to use the modified method than to merely reduce the time step by half.

Figure 8 shows the results for compression and shear. Comparing these results with those in Fig. 5 we observe that the modified method accurately follows the hardening during the compression phase. The curve for the shear stress is not presented because the results are nearly identical to those in Fig. 5b.

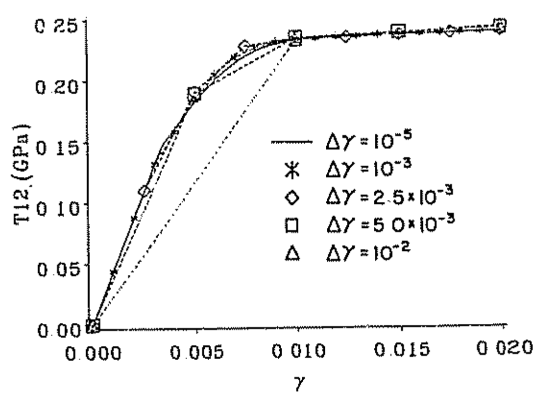

Figure 7
Simple Shear: Values of the shear stress calculated for the hardening material characterized by (4.8c) using the modified estimate of hardening. The influence of changing the step size $\Delta\gamma$ is shown for the shearing rate $\dot{\gamma} = 10^{-4}\,\text{s}^{-1}$

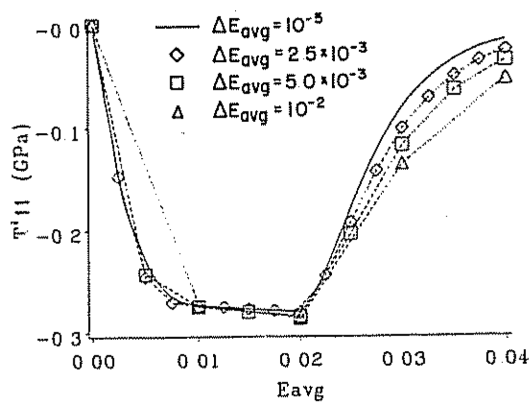

Figure 8
Compression-Shear: Values of the deviatoric stress calculated for the hardening material characterized by (4.8c) using the modified estimate of hardening. The influence of changing the step ΔE_{avg} is shown for the compression rate $\dot{a} = -10^{-4}\,\text{s}^{-1}$ and the shearing rate $\dot{\gamma} = 10^{-4}\,\text{s}^{-1}$.

8. Conclusions

A simple unconditionally stable numerical procedure for time integration of the flow rule for large plastic deformation of an elastic-viscoplastic metal has been developed. Specific attention has been focused on a unified set of constitutive equations which does not use the notion of a yield function. Also, an analytical solution has been obtained for large deformation simple shear at constant shear rate which is valid for a general elastic-viscoplastic metal exhibiting isotropic elastic response. Comparison of the numerical solution of simple shear with the analytical solution indicates that the procedure developed here accurately predicts the value of the Cauchy shear stress even for extremely large integration steps. When these large integration steps are used errors occur in the prediction of the normal stresses. However, these errors are often negligible because the normal stresses are approximately two orders of magnitude lower than the shear stress.

Specific equations of a rate insensitive metal characterized by a yield function as well as a rate sensitive metal characterized by an overstress model have been considered to show how the procedure may be implemented for other models.

Finally, in order to compare the present integration procedure with one currently used for stiff differential equations [13], we reconsidered the example of simple shear. Specifically, for small deformations, the equations recorded in the appendix of [12] yield

$$T_{12} = \mu_0 \gamma_e, \quad \gamma_e(t_2) = \gamma_e(t_1) + \Delta\gamma_e, \tag{8.1a,b}$$

$$\Delta\gamma_e = [\gamma(t_2) - \gamma(t_1) - \Delta t \Gamma \gamma_e]/[1 + \bar{\eta}\ \Delta t \Gamma\{1 + n(Z/\sigma_e)^{2n}\}], \tag{8.1c}$$

where $\bar{\eta}$ is a constant; Γ and σ_e are defined by (2.11c,d); and γ_e, Γ, z, σ_e in (8.1c) take their values at the beginning of the time step ($t = t_1$). The value of $\bar{\eta}$ is taken in the range ($1/2 \le \bar{\eta} \le 1$) for stability [31].

Figure 9 shows the shear stress T_{12} calculated for $\dot{\gamma} = 10^{-4}\,\mathrm{s}^{-1}$, $\bar{\eta} = 1$, and three different example materials specified by (4.8a) and

$$n = 5.0, \quad \kappa = Z_1, \quad Z_1 = 0.654\ \mathrm{GPa}, \quad Z_3 = 0, \tag{8.2a}$$

$$n = 10.0, \quad \kappa = Z_1, \quad Z_1 = 0.541\ \mathrm{GPa}, \quad Z_3 = 0, \tag{8.2b}$$

To isolate the effect of rate sensitivity, the values of Z_1 in (8.2a,b) were determined using the formula (4.15) which ensures that the flow stress for $\dot{\gamma} = 10^{-4}\,\mathrm{s}^{-1}$ is the same for all three materials. Using Tables 1 and 3 of [9] we observe that $n = 1, 5, 10$ are representative of Ti, Al 6061-T6, and Al 2024-0, respectively. It is obvious from Fig. 9 that the accuracy decreases significantly as the material becomes more rate insensitive (n increases) and that oscillations can occur which make the predictions unusable. In contrast,

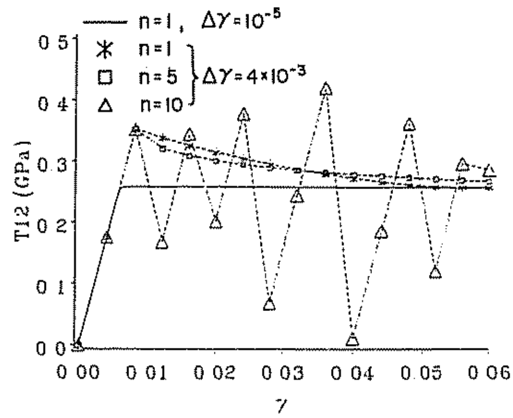

Figure 9
Simple Shear: Values of the shear stress calculated for the material characterized by (4.8a) using the solution procedure proposed in [13]. The influence of decreasing the material rate sensitivity (increasing n) is shown for the shearing rate $\dot{\gamma} = 10^{-4}\,\mathrm{s}^{-1}$ with $\Delta\gamma = 0.004$.

we recall from Fig. 2 that the procedure presented here produces accurate results even for a large step ($\Delta\gamma = 0.1$) and an extremely rate insensitive material ($n = 100$). Furthermore, we note that for this procedure the numerical effort required in the limit of nearly rate insensitive response is not greater than that required for rate sensitive response, even though the flow rule for elastic viscoplastic response becomes extremely stiff when the material response is nearly rate insensitive.

Addendum

Just before this paper was submitted for publication the author received a preprint [32] which discusses a numerical procedure for viscoplasticity which also requires determination of the root of a scalar equation (see 3.15). However, the constitutive equations considered here are significantly different from those discussed in [32].

Appendix: small deformation formulation

For analyzing small deformations it is convenient to introduce the total, plastic, and elastic strains $\mathbf{E}, \mathbf{E}_p, \mathbf{E}_e$, respectively, by

$$\mathbf{E} = (1/2)(\mathbf{C} - \mathbf{I}), \quad \mathbf{E}_p = (1/2)(\mathbf{C}_p - \mathbf{I}), \quad \mathbf{E}_e = (1/2)(\mathbf{C}_e - \mathbf{I}) \qquad \text{(A1a,b,c)}$$

It follows from (2.1b,c) that for small deformations and small strains

$$\mathbf{M}_p = \mathbf{I} + \mathbf{E}_p, \quad \mathbf{M}_p^{-1} = \mathbf{I} - \mathbf{E}_p, \quad \mathbf{E}_e = \mathbf{E} - \mathbf{E}_p, \qquad \text{(A2a,b,c)}$$

$$\mathbf{C}_p^{-1} = \mathbf{I} - 2\mathbf{E}_p, \quad \mathbf{B}_e = \mathbf{I} + 2\mathbf{E}_e, \quad \mathbf{B}_e^{-1} = \mathbf{I} - 2\mathbf{E}_e, \qquad \text{(A2d,e,f)}$$

Neglecting quadratic terms in the strains and using the equations (4.2), (5.3), (5.4) of [12] the constitutive equation (2.9) reduces to

$$\mathbf{T}' = 2\mu_0 \mathbf{E}_e' = 2\mu_0(\mathbf{E}' - \mathbf{E}_p), \qquad \text{(A3)}$$

where $\mathbf{E}_e'$ and $\mathbf{E}'$ are the deviatoric parts of $\mathbf{E}_e$ and $\mathbf{E}$, respectively, and μ_0 is the reference value of the shear modulus. The tensor $\mathbf{A}$ in (2.11a) becomes

$$\mathbf{A} = 2(\mathbf{E}' - \mathbf{E}_p), \tag{A4}$$

so the flow rule (2.10a) reduces to

$$\dot{\mathbf{E}}_p = \Gamma(\mathbf{E}' - \mathbf{E}_p) = (\Gamma/2\mu_0)\mathbf{T}'. \tag{A5}$$

Furthermore, $\mathbf{C}_p^{-1}$ in (2.10c) and (2.11f,g,h) may be set equal to $\mathbf{I}$.

Now, the method of section 3 suggests that the flow rule (A5) be solved implicitly over the time interval $[t_1, t_2]$ such that (see 3.1)

$$\mathbf{E}_p(t_2) - \mathbf{E}_p(t_1) = \Delta t \Gamma[\mathbf{E}'(t_2) - \mathbf{E}_p(t_2)], \tag{A6}$$

where Γ in (A6) and (2.11c) is evaluated at the end of the time step ($t = t_2$). Furthermore, since (A5) requires plastic strain $\mathbf{E}_p$ to evolve in the direction of deviatoric strain $\mathbf{E}'$ we assume that $\mathbf{E}_p(t_2)$ may be expressed in the alternative form (see 3.8)

$$\mathbf{E}_p(t_2) = \mathbf{E}'(t_2) - \lambda[\mathbf{E}'(t_2) - \mathbf{E}_p(t_1)], \tag{A7}$$

where λ is a scalar to be determined. Thus (see 3.9)

$$\mathbf{E}_p(t_2) - \mathbf{E}_p(t_1) = (1 - \lambda)[\mathbf{E}'(t_2) - \mathbf{E}_p(t_1)], \tag{A8a}$$

$$\mathbf{E}'(t_2) - \mathbf{E}_p(t_2) = \lambda[\mathbf{E}'(t_2) - \mathbf{E}_p(t_1)]. \tag{A8b}$$

Also, the effective stress σ_e in (2.11d) at the end of the time step is given by (see 3.12)

$$\sigma_e^2 = 6\mu_0^2[\mathbf{E}'(t_2) - \mathbf{E}_p(t_2)] \cdot [\mathbf{E}'(t_2) - \mathbf{E}_p(t_2)] = \lambda^2 \bar{\sigma}_e^2, \tag{A9a}$$

$$\bar{\sigma}_e^2 = 6\mu_0^2[\mathbf{E}'(t_2) - \mathbf{E}_p(t_1)] \cdot [\mathbf{E}'(t_2) - \mathbf{E}_p(t_1)], \tag{A9b}$$

where $\bar{\sigma}_e$ is the effective stress that would be calculated if the response were elastic. It follows by using (A8), (A9) and the form (2.11c) that the approximation (A6) of the flow rule reduces to the scalar equation (3.13), which is satisfied by solving for the root of (3.15).

Finally, we note that for the small deformation theory the rate of plastic dissipation (2.7g) becomes

$$\varrho_0 \theta \xi' = \mathbf{T}' \cdot \dot{\mathbf{E}}_p, \tag{A10}$$

which is the usual expression for the rate of plastic work.

References

[1] A. E. Green and P. M. Naghdi, *A general theory of an elastic-plastic continuum*. Arch. Rat. Mech. Anal. *18*, 251–281 (1965).

[2] L. E. Malvern, *The propagation of longitudinal waves in a bar of material exhibiting a strain-rate effect*. ASME J. Appl. Mech. *18*, 203–208 (1951).

[3] P. Perzyna, *Fundamental problems in viscoplasticity*. in *Advances in Applied Mechanics*, vol. 9, pp. 243–277. Academic Press, New York 1966.

[4] A. K. Miller, *Unified Constitutive Equations for Creep and Plasticity*, Elsevier Applied Science, England 1987.

[5] G. E. Dieter, *Mechanical Metallurgy*, McGraw-Hill, Sec. 9-6, New York 1976.

[6] S. R. Bodner and Y. Partom, *A large deformation elastic-viscoplastic analysis of a thick-walled spherical shell* ASME J. Appl. Mech. *39*, 751–757 (1972).

[7] S. R. Bodner and Y. Partom, *Constitutive equations for elastic-viscoplastic strain-hardening materials* ASME J. Appl. Mech. *42*, 385–389 (1975).

[8] S. R. Bodner, *Evolution equations for anisotropic hardening and damage of elastic-viscoplastic materials, Plasticity Today—Modelling, Methods and Applications* (Eds. A. Sawczuk and G. Bianchi), pp. 471–482. Elsevier, London 1985.

[9] S. R. Bodner, *Review of a unified elastic-viscoplastic theory*, In *Unified Constitutive Equations for Creep and Plasticity* (Ed. A. K. Miller). Elsevier Applied Science, England 1987.

[10] M. B. Rubin, *An elastic-viscoplastic model for large deformation*. Int. J. Engng. Sci. *24*, 1083–1095 (1986).

[11] M. B. Rubin, *An elastic-viscoplastic model for metals subjected to high compression*. ASME J. Appl. Mech. *54*, 532–538 (1987).

[12] M. B. Rubin, *An elastic-viscoplastic model exhibiting continuity of solid and fluid states*, Int. J. Engng. Sci. *25*, 1175–1191 (1987).

[13] M. B. Kanchi, O. C. Zienkiewicz and D. R. Owen, *The viscoplastic approach to problems of plasticity and creep involving geometric nonlinear effects*. Int. J. Num. Meth. Engng. *12*, 169–181 (1978)

[14] M. L. Wilkins, *Calculations of elastic-plastic flow*. In *Methods in Computational Physics*, vol. 3, pp. 211–263. Academic Press, New York 1964.

[15] G. Maenchen and S. Sack, *The tensor code*. In *Methods in Computational Physics*, vol. 3. Academic Press, New York (1964).

[16] R. D. Krieg and S. W. Key, *Implementation of a time independent plasticity theory into structural computer programs*. In *Constitutive Equations in Viscoplasticity: Computational and Engineering Aspects* (Eds. J. A. Stricklin and K. J. Sacalski), AMD-20, pp. 125–137. ASME, New York 1976.

[17] M. B. Rubin, *The Significance of nonhydrostatic distortional strain for anisotropic elastic-plastic metals* (submitted for publication 1988).

[18] M. B. Rubin, *An elastic-plastic model which remains form invariant under change of the reference configuration* (submitted for publication 1989).

[19] V. A. Lubarda and E. H. Lee, *A correct definition of elastic and plastic deformation and its computational significance*. ASME J. Appl. Mech. *48*, 35–40 (1981).

[20] A. E. Green and P. M. Naghdi, *Some remarks on elastic-plastic deformation at finite strain*. Int. J. Engng. Sci. *9*, 1219–1229 (1971).

[21] E. H. Lee, *Elastic-plastic deformation at finite strains*. ASME J. Appl. Mech. *36*, 1–6 (1969).

[22] M. B. Rubin, *The significance of pure measures of distortion in nonlinear elasticity with reference to the Poynting problem*. J. Elasticity *20*, 53–64 (1988).

[23] P. J. Flory, *Thermodynamic relations for high elastic materials*. Trans. Faraday Soc. *57*, 829–838 (1961).

[24] J. C. Simo, R. L. Taylor and K. S. Pister, *Variational and projection methods for the volume constraint in finite deformation elasto-plasticity*. Computer Meth. Appl. Mech. Engng. *51*, 177–208 (1985).

[25] A. E. Green and P. M. Naghdi, *On thermodynamics and the nature of the second law*. Proc. Royal Soc. Lond., Vol. A *357*, 253–270 (1977).

[26] A. E. Green and P. M. Naghdi, *The second law of thermodynamics and cyclic processes*. ASME J. Appl. Mech. *45*, 487–492 (1978).

[27] R. J. Clifton, *Dynamic plasticity*. ASME J. Appl. Mech. *50*, 941–952 (1983).

[28] R. D. Krieg and D. B. Krieg, *Accuracies of numerical solution methods for the elastic-perfectly plastic model*. ASME J. Pressure Vessel Tech. *99*, 510–515 (1977).

[29] P. M. Naghdi and J. A. Trapp, *The significance of formulating plasticity theory with reference to loading surfaces in strain space*. Int. J. Engng. Sci. *13*, 785–797 (1975).

[30] W. C. Moss, *On the computational significance of the strain space formulation of plasticity theory*. Int. J. Numer. Meth. Engng. *20*, 1703–1709 (1984).

[31] T. J. R. Hughes and R. L. Taylor, *Unconditionally stable algorithms for quasi-static elasto/visco-plastic finite element analysis*. Computers and Structures *8*, 169–173 (1978).

[32] D. J. Steinberg and C. M. Lund, *A constitutive model for strain rates from 10^{-4} to $10^{6}\,s^{-1}$*, UCRL-98281 Preprint, Lawrence Livermore National Laboratory, Livermore 1988.

Abstract

A simple unconditionally stable numerical procedure for time integration of the flow rule for large plastic deformation of an elastic-viscoplastic metal is developed. Specific attention is focused on a unified set of constitutive equations which represents a generalization (for large deformation and thermomechanical response) of the Bodner-Partom model [6, 7]. An analytical solution is obtained for large deformation simple shear at constant shear rate. Numerical examples of simple shear, a corner test exhibiting the transition from uniaxial compression to shear, and simple tension are considered which demonstrate the stability and accuracy of the procedure. It is shown that the same procedure can be used for a rate insensitive metal characterized by a yield function as well as for a rate sensitive metal characterized by an overstress model. Finally, an appendix is provided which records the basic equations associated with the small deformation theory.

(Received: June 2, 1988)